minerals

MDPI

Article

Mineralogy and Selenium Speciation Analysis of Early Cambrian Selenium-Rich Black Shale in Southern Shaanxi Province, China

Caixia Feng *, Shen Liu, Wenlei Song, Chenhui Hou and Yanhong Yang

State Key Laboratory of Continental Dynamics, Department of Geology, Northwest University, Xi'an 710069, China; liushen@nwu.edu.cn (S.L.); wlsong@nwu.edu.cn (W.S.); 202121909@stumail.nwu.edu.cn (C.H.); xvdongzhe@stumail.nwu.edu.cn (Y.Y.)
* Correspondence: fengcaixia@nwu.edu.cn; Tel.: +86-18229079027

Abstract: Selenium (Se) is an essential trace element for humans and animals, and an excess of or deficiency in Se is harmful to health. Research on the selenium enrichment zone began in the late 1970s in Shuang'an, Ziyang, southern Shaanxi Province. Naore village is only one selenosis area in Shuang'an, Ziyang, China. Different scholars have conducted systematic studies on the occurrence of selenium, its organic geochemistry and biomarkers, and its content and enrichment patterns in this area. This study applied the TIMA (TESCAN integrated mineral analyzer) for the first time to conduct detailed mineralogical work. The minerals included quartz, carbonate minerals (calcite and dolomite), feldspar (plagioclase, albite, and orthoclase), biotite and muscovite, clay minerals (chlorite and kaolinite), hematite, pyrite, and accessory minerals (almandine, olivine, zircon, and apatite) in Naore village, Ziyang, Shaanxi Province. The ATi index (100 × apatite/(apatite + tourmaline)) is used to determine the source of heavy minerals and the degree of heavy minerals' weathering. The content POS (100 × (pyroxene + olivine + spinel)/transparent heavy mineral) of olivine, pyroxene, and spinel in heavy minerals can reflect the contribution of basic and ultrabasic rocks in the source area. The ATi and POS indexes for the heavy minerals in the research area were 91.83~99.96 and 0.01~18.75, respectively, reflecting the abundance of volcanic rock material in their source. In addition, the migration, transformation, bioavailability, and toxicity of selenium in the environment are closely related to its species. The species of selenium in various selenium-rich areas (Naore, Wamiao, and Guanquan) mainly include unusable residues and organic forms, followed by humic-acid-bound selenium. The proportions of water-soluble, exchangeable, and carbonate-bound selenium are relatively small, and the proportion of Fe-Mn oxide-bound selenium is the lowest.

Keywords: mineralogy; selenium speciation; early Cambrian; Se-rich black shale; southern Shaanxi province; China

Citation: Feng, C.; Liu, S.; Song, W.; Hou, C.; Yang, Y. Mineralogy and Selenium Speciation Analysis of Early Cambrian Selenium-Rich Black Shale in Southern Shaanxi Province, China. *Minerals* **2024**, *14*, 612. https://doi.org/10.3390/min14060612

Academic Editor: Basilios Tsikouras

Received: 29 April 2024
Revised: 5 June 2024
Accepted: 13 June 2024
Published: 15 June 2024

1. Introduction

Black shales are characterized by their abundance of organic matter, sulfide minerals, and high concentrations of trace elements (e.g., V, U, Cu, Mn, Ba, Cd, Ni, Zn, Mo, Pb, and REEs) [1–6]. At the same time, their formation is also related to global catastrophes, such as biological explosions [7], extraterrestrial events [8–11], volcanic events [12], etc. Early Paleozoic black shales are widely distributed in southern China, e.g., the Niutitang Formation of the Cambrian Series [13], the Miaopo Formation of the Middle Ordovician [9], the Wufeng Formation of the Upper Ordovician [14], and the Longmaxi Formation of the Lower Silurian [15]. These formations are mostly associated with near-global oceanic anoxic events [13]. Therefore, research on black shales has extremely important geological significance for paleontology, event geology, stratigraphy, mineral deposit science, and oil and gas geology [7,8,16–20].

Research has shown that black shales are enriched with dispersed elements of Se: (1) the enrichment of polymetallic elements of the Early Cambrian Niutitang Formation in Zunyi, Guizhou, southern China [19,21], and Xiangxi, western Hunan, China [22]; (2) the selenium enrichment of the Lower Cambrian Lujiaping Formation in Shuang'an, Ziyang, the southern Qinling Mountains, China [23,24]; (3) the Larma Se-Au deposit in the Cambrian Taiyangding Group [25]; and (4) the independent selenium deposit in Yutangba of Enshi Shuanghe, western Hubei, in the Permian Maokou Formation [20,26,27].

The mineralogical study of selenium began in the 1950s, e.g., purple-gray needle-shaped natural selenium (Se) [28], ferroselite (FeS_2) and clausthalite (PbSe) [29], and so on. Significant progress was made in mineralogical research starting in the 1980s: (1) the discovery of natural selenium minerals (Se) in the same carbonaceous layer in the geological environment [30]; (2) antimonselite (Sb_2Se_3) in U-Hg-Mo polymetallic deposits in Guizhou, southern China [31]; (3) selenio-sulfantimonide ($Sb_2(S,Se)_3$) and selenio-copper antimony sulfide ($Cu_3Sb(S, Se)_4$) in the Se-Au deposits in Laerma, northwestern China [32]; (4) klockmannite (CuSe), chalcomenite ($CuSeO_3 \cdot 2H_2O$), and krutaite ($CuSe_2$) in Yutangba, Hubei, China [33]; and (5) tiemannitet (HgSe), selenio-sulfantimonide ($Sb_2(S,Se)_3$), selenio-copper antimony sulfide ($Cu_3Sb(S, Se)_4$), ferroselite (FeS_2), a small group of clausthalite (PbSe), antimonselite (SbSe), Scderholmite (NiSe), and berzelianite (Cu_2Se) in the Se-Au deposits in Laerma, northwestern China [34].

In addition, geochemistry applies chemical principles and experiments to understand earth science and engineering problems [35]. Many scholars use continuous extraction and analytical chemistry methods to distinguish the forms of selenium in the detection environment based on its environmental significance [36–39]. There are generally the water-soluble, exchangeable, organically bound (alkali-soluble), elemental, carbonate-bound (acid-soluble), sulfide-/selenide-bound, and residual states of selenium [39]. Moreover, the water-soluble and exchangeable states are usually considered biologically available selenium [38,40,41]. In the ecological geochemical cycle of selenium, the state of its occurrence controls its environmental geochemical behavior, including its water solubility, toxicity, bioavailability, redox state, etc., which in turn affects its ecological benefits [42].

Research on the selenium enrichment zone in Shuang'an, Ziyang, Shaanxi Province began in the late 1970s. Different scholars have conducted systematic studies on the occurrence of selenium, its organic geochemistry and biomarkers, and its content and enrichment patterns [43–46]. Naore village is only one of the selenosis areas in the Shuang'an area [47]. The selenium content of the corn in Naore village is 6.6 mg/kg [48], and the horsebeans reach 48.84 mg/kg of Se [43]. The selenium contents of the soil in these fields are 15.74 mg/kg [43] and 26 mg/kg [49]. The village people consume selenium-enriched crops from these fields. Previous studies on mineralogy and selenium in southern Qinling found the following: (1) The black rock series in the Qinling Mountains is made up of carbonaceous argillite, carbonaceous siliceous argillite, marl, stone coal, and carbonaceous limestone; additionally, phosphatic nodules, pyrite, and barite are always found in these rocks [50]. (2) Systematic studies on the Se content of different lithologies from this area have indicated that the Lower Cambrian, carbonaceous, and siliceous strata host the highest levels of Se [24]. (3) By combining studies on ore characteristics, performing analyses of mineralization elements, and conducting electron probe analyses, the contents of Fe, Cu, Zn, and the other metallic elements in carbonaceous shale were determined [51]. (4) The relationship between selenium and the mineral content in Ziyang rocks showed a negative correlation between Se and both quartz and sodium feldspar. Illite is a clay mineral with a strong adsorption capacity for selenium, and pyrite is involved in an important mechanism for selenium enrichment in rocks [52]. (5) The content of organic matter is high in the Lower Cambrian, Ziyang, and there are two modes of occurrence: dispersed organic matter and aggregated organic matter. The relationship between dispersed organic matter and clay minerals is close. The average total organic carbon (TOC) is affected by lithologic differences and the pyrite content and type [53].

Based on the above, it can be seen that previous studies on the occurrence of minerals in the Se-rich black shale and soil in southern Qinling have mainly focused on using microscopes [24,50] and electron probes (EPMAs) [51]; mineralogical research work has been relatively weak. Due to the high spatial resolution and built-in mineralogical spectrum dataset, a TIMA could identify and quantify minerals with a grain size from the mm to μm scale, including the mineral abundance [54]. In order to determine the specific composition, content, particle size, element distribution, and occurrence status of minerals accurately, we selected the TIMA (TESCAN integrated mineral analyzer), a fully automatic comprehensive mineral analysis system based on scanning electron microscopy (SEM) and energy-dispersive X-ray (EDX) analysis, to conduct detailed mineralogical work on the selenium-rich black shale and soil of Naore village, Ziyang area. In addition, the migration, transformation, bioavailability, and toxicity of selenium in the environment are closely related to its concentration and species, which then influence the Se content and species in plants and human bodies [52]. Therefore, studying Se speciation in the rock–soil system is very important for understanding the eco-geochemical cycle of Se, which is beneficial for reasonably utilizing Se resources.

Considering this background, the purposes of this study were as follows: (1) determine the detailed mineral composition of the rock and soil in Naore village and (2) assess the relationship between Se content and species in the rock and soil of Naore, Wamiao, and Guanquan villages, Ziyang. The research results will help reveal further biogeochemical effects of Se and the relationship between Se and other elements, lay the foundation for geological health surveys, and provide a theoretical reference and technical support for Se resource exploitation.

2. Geological Background

Ziyang County is located in the southern part of Shaanxi Province, China (Figure 1a). Geologically, the region belongs to the Qinling orogenic belt, which is a major tectonic boundary separating the North China Block from the South China Block [24]. According to the tectonic evolutionary history of the Yangtze Plate, there was a southward subduction event at the edge of the Yangtze landmass in the Neoproterozoic. With the end of the subduction, the North Daba Mountains area evolved into a passive continental margin in the northern part of the Yangtze landmass during the Cambrian period [55,56]. The thickness of the Cambrian sediments in the Daba Mountain area underwent a thin (1480–1625 m)–thick (2246 m)–thin variation from the southern Daba Mountain area to the Maoba–Zhenping area and then to the Ziyang–Pingli area [57]. The variation pattern of the thickness of this stratum also reflected the fact that the main thrust faults in the Early Paleozoic era controlled the strong differential sedimentation of the two sides of the strata through synsedimentary extensional deformation [57,58].

The Se-enriched Lower Cambrian strata outcrop on Daba Mountain extends over the whole county (Figure 1b) [47,59]. There are three NW–SE-trending major faults (Yuehe Fault Zone, Hongchunba Fault Zone, and Dabashan Deep Fault Zone) distributed from north to south in the research area (Figure 1b) [47,50]. The fault zones are characterized by anticlines and synclines, and a large number of black rock-type deposits are distributed along the fault zones, such as plagioclase, barite, and barium calcite deposits (Figure 1b). The black shales in the research area belong to the Lower Cambrian black rock series of the Qinling Mountains, which is an important ore-forming rock series in northern China. It is rich in carbonaceous or interbedded coal, with rare fossils and very thick siliceous rocks [60]. The distribution strata are mainly the Jianzhuba Formation and the Lujiaping Formation (Figure 1b), and the orientation of the strata is consistent with the direction of the fault. The most concerning area of selenosis in the Shuang'an countryside of Ziyang County is very small and limited to Naore village (Figure 1c) [43].

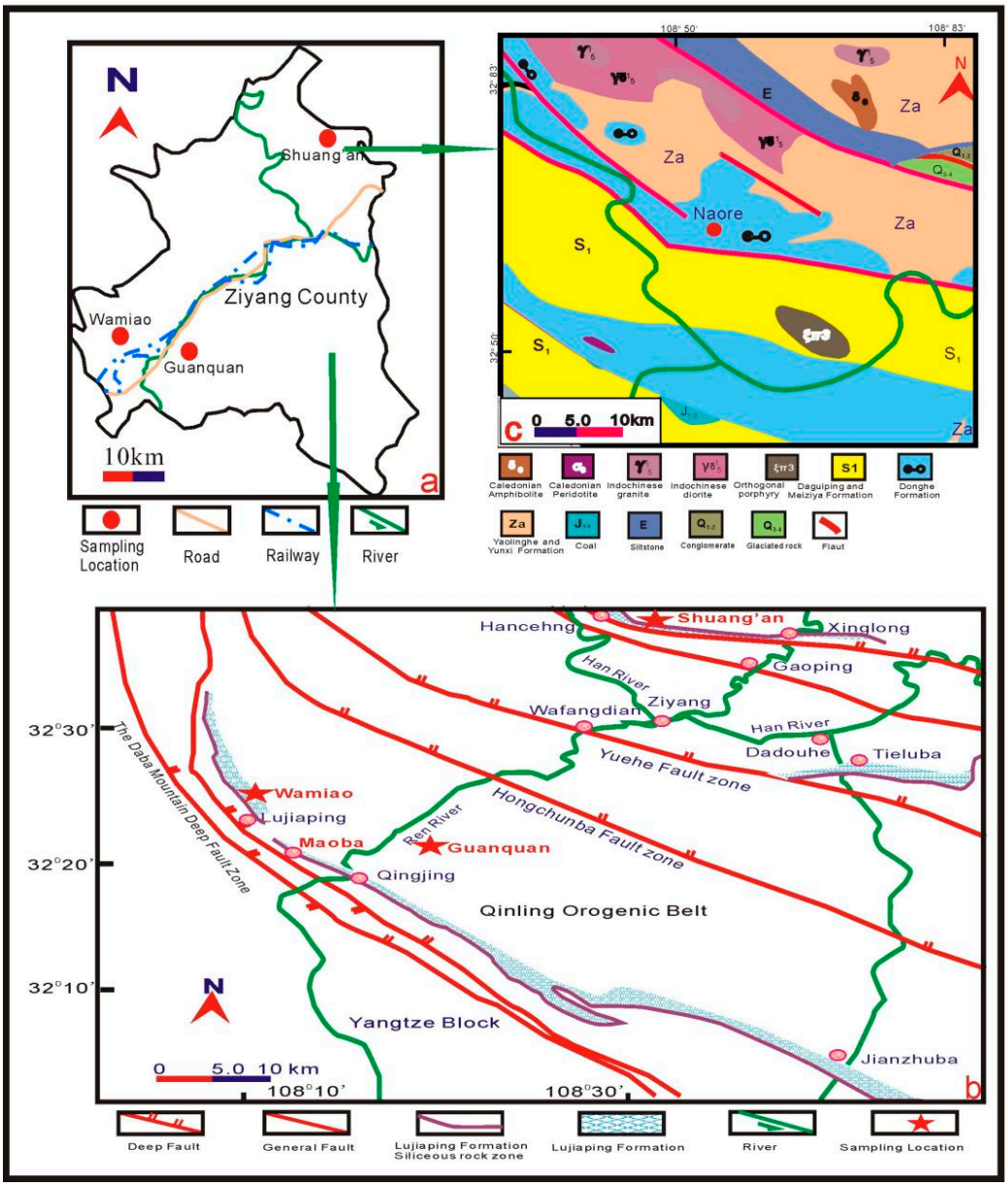

Figure 1. Geological map of study area. (**a**) Location of study area (modified from Tian et al. [44]); (**b**) distribution of Lower Cambrian Lujiaping Formation and Fault in study area (modified from Luo et al. [47]; Wang et al. [61]; and Zhao et al. [53]); (**c**) geological sketch map of Naore village (modified from Hou et al. [62]).

The main rocks of the Lujiaping Formation are carbonaceous siliceous rock (Figure 2a–c), slate (Figure 2d), sapropelite (Figure 2e), carbonaceous shale (Figure 2f), and a small amount of carbonaceous siltstone, partially interbedded with phosphorite and stone coal, with a thickness of about 700–900 m. In addition to the obvious enrichment in Se, this formation is also enriched with elements such as Ba, V, and Cr, as well as a large amount of barite and toxic stone coal. The Jianzhuba Formation is mainly composed of dark-gray limestone containing argillaceous micrite, with a thickness of 170–300 m [24,53,61,62].

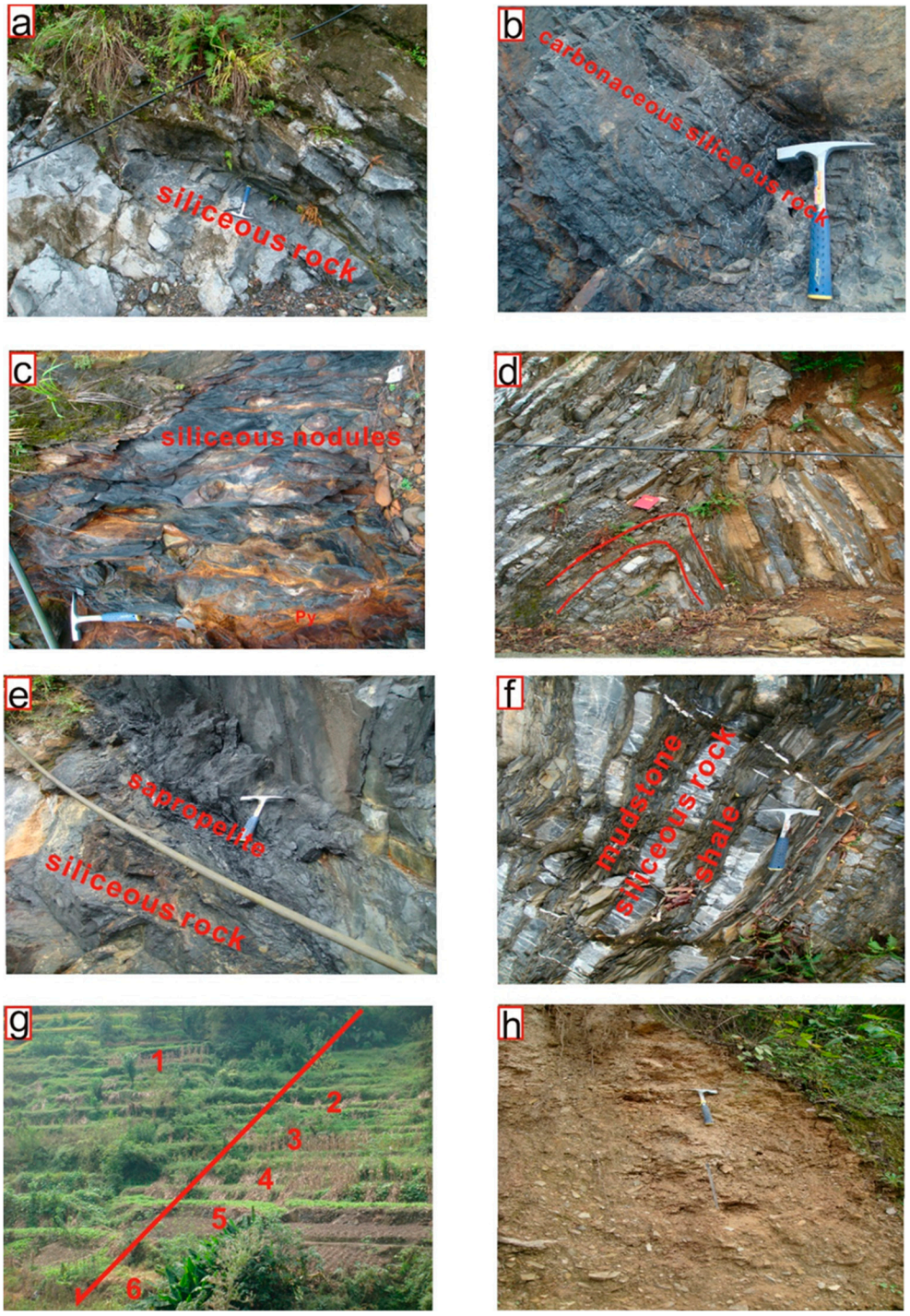

Figure 2. Photos of various occurrences and lithology of Se-rich black shale in study area. (**a**) Thick and thin interbedded siliceous rock; (**b**) carbonaceous siliceous rock, with high organic content, interspersed with dolomite veins; (**c**) carbonaceous siliceous rock, with high organic content; (**d**) tight fold of slate and shale; (**e**) sapropelite interbedded with siliceous rock; (**f**) mudstone interbedded with siliceous rock and shale; (**g**) distribution of soil-sampling points from north to south; (**h**) typical yellow-brown soil profile.

3. Sampling and Analytical Methods

3.1. Field Sampling and Sample Preparation

Most of the samples collected for this study came from the Lower Cambrian Lujiaping Formation. The rock and soil samples investigated herein were collected from Naore,

Wamiao, and Guanquan villages in Ziyang, Ankang, Shaanxi Province, China. The sampling points were distributed on the rock layers and farmlands around the village. A total of 20 rock and 12 soil samples (from north to south; Figure 2g,h) were collected.

During the process of collecting samples, the surface-oxidized ore was knocked off, and fresh, representative samples that were not exposed were selected for microscopic (rock) mineralogical observations and TIMA analysis.

The samples were cleaned with tap water to wipe off all contaminants, washed again with deionized water, stored under dry conditions, and powdered with an agate mill. The soil samples were dried naturally, and any plant fragments and roots were removed. Following collection, the samples were taken to the laboratory for processing.

3.2. Mineral Analysis

Fresh samples were selected for grinding thin sections, and separate sections were probed for petrological and mineralogical identification.

Approximately 2 g of the rock samples was sliced, and the soil samples were compacted and embedded in resin to form a target for machine testing. A scanning electron microscopy analysis was performed by using the mineral liberation analysis (MLA) in situ method [63,64], which did not involve particle size screening or heavy-mineral sorting. This method can prevent the loss of some heavy minerals during manual screening and washing and can also better preserve mineral particles such as quartz and feldspar. The exported data included but were not limited to the following: the mineral type, the size of each mineral phase and the count, the size of each mineral particle and the count, the type of mineral phase contained, etc. Mineral phase particles with a size greater than 5 μm were identified.

The testing work of the mineral quantitative analysis system (TIMA) was completed at the Continental Dynamics Laboratory of the Department of Geology, Northwestern University. The testing system was mainly composed of a TESCAN MIRA 3 scanning electron microscope equipped with 9 detectors, namely, 4 EDAX (Element 30) high-throughput silicon drift detectors (detection area of 30 mm^2), BSE and SE detectors inside the mirror tube, an ultrafast YAG scintillator BSE detector, a secondary electron EverhartThornley detector, and a scalable cathode fluorescence detector (350–850 nm). The testing mode was the high-vacuum mode, with an acceleration voltage of 25 kV, a current of 9 nA, and a working distance of 15 mm. The current and BSE signal strengths were calibrated using a platinum Faraday cup automatic program, and the EDS signal was calibrated by using Mn standard samples. In the test, the lattice mode of the dissociation analysis was used, with an X-ray count of 1000 for each point and a pixel spacing of 3 μm [54].

3.3. Se Content and Speciation Analysis

The samples were analyzed for whole-rock and soil Se element concentrations by using an atomic fluorescence spectrometer (AFS; AFS-933; Jitian Beijing, China) on the Xi'an E-test platform, Ltd., in Xi'an, China. The powdered samples were weighed to 0.2 g and placed in a 50 mL beaker with 15 mL of HNO_3 and 3 mL of $HClO_4$ and then heated for 2 min. Next, 5 mL of HCl was added, and the low temperature was increased until the mixture was slightly boiling. Then, the mixture was cooled and maintained at a constant volume in a 25 mL colorimetric tube. After dissolution, the samples were tested by using the AFS; the analytical accuracy and precision were within ±5% [65].

The samples were analyzed for Se speciation by using the five-step sequential extraction method by Tessier et al. [66] and Qu et al. [67] on the Xi'an E-test platform by using the PE-OPTIMA 7000 full-spectrum direct-reading inductively coupled plasma emission spectrometer as follows:

1. Organically bound Se: Amounts of 8 mL of 5% $K_2S_2O_8$ and 2 mL of concentrated HNO_3 were added to each remaining soil sample, and the vial was heated for 3 h in a water bath at 95 °C. The tube was intermittently shaken from time to time.

2. Iron (Fe)/manganese (Mn) oxide-bound Se: An amount of 10 mL of 2.5 mol/L HCl was added to the remaining soil. The capped vials were then heated in a water bath at 90 °C for 50 min. The centrifuge vials were also shaken intermittently.
3. Carbonate-bound Se: An amount of 10 mL of 0.7 mol/L KH_2PO_4 (pH of 5.0) was added to the above tube, and the tube was shaken at 200 rpm and 25 °C for 4 h.
4. Exchangeable Se: An amount of 10 mL of 1.0 mol/L magnesium chloride ($MgCl_2$) was added to the above tube, and the tube was shaken at 200 rpm and 25 °C for 4 h.
5. Residual Se: The residuals were transferred into Teflon crucibles with 8 mL of concentrated HNO_3 and 2 mL of concentrated $HClO_4$. The crucibles were covered and heated to 170 °C in a sand bath until the soil appeared white or gray. After acid digestion, the solution was transferred to a 25 mL volumetric flask with deionized water.

4. Results

4.1. Microphysiography of Samples

The black rock series can be divided into siliceous shale (quartz + feldspar > 50.0%, clay minerals < 40.0%, and carbonate minerals < 30.0%), clay-type shale (quartz + feldspar < 50.0%, clay minerals < 40.0%, and carbonate minerals < 30.0%), and carbonate shale (carbonate minerals > 30.0%) [68,69]. The average content of brittle minerals (siliceous minerals such as quartz, feldspar, etc., and carbonate minerals such as calcite and dolomite) in Naore was over 80% (the content of quartz + feldspar was > 50.0%, and that of carbonate minerals was about 26%), and the content of clay minerals was relatively low, which indicated that the rock type in the study area was mainly the siliceous shale type. The detailed petrography under the microscope is shown in Figure 3.

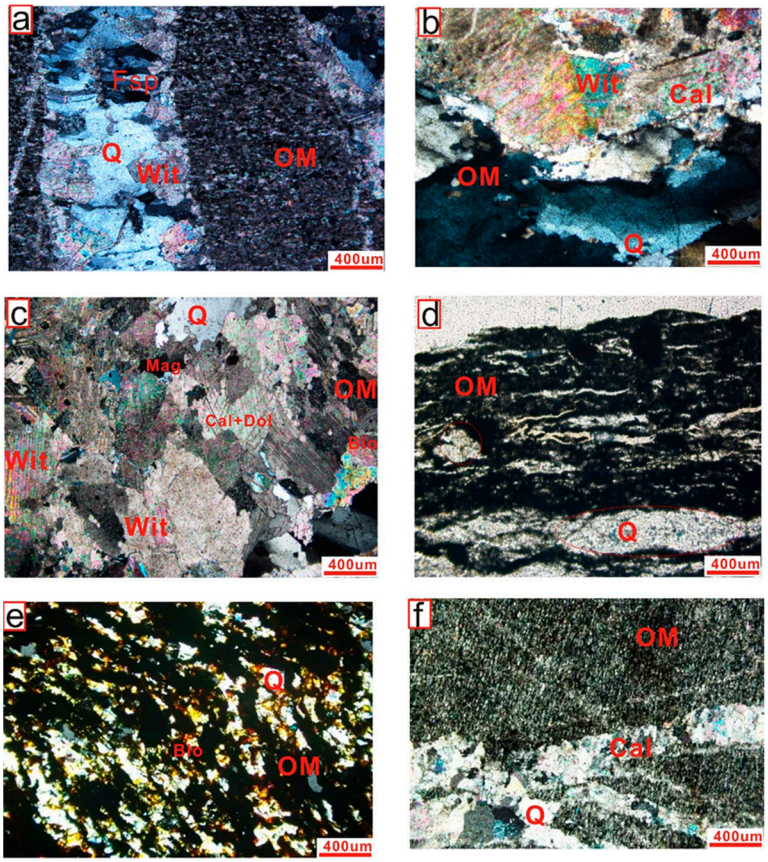

Figure 3. Microscope photos from Naore village, Ziyang, southern Shaanxi, China. (**a**) Siliceous slate: muddy fine-grained structure mainly composed of quartz, feldspar, and witherite. (**b**) Calcareous and carbonaceous slate: fine-grained structure mainly composed of quartz, calcite, witherite, and

organic matter. (**c**) Calcareous slate: fine-grained structure; the mineral composition is mainly quartz, calcite, witherite, dolomite, and organic matter, with small amounts of biotite and magnetite. (**d**) Stone coal: oriented black organic matter and colorless quartz bands, indicating low-grade metamorphism. (**e**) Siliceous shale: the mineral composition is mainly quartz and organic matter, black carbon, and quartz stripes with directional interlacing, interspersed with brown biotite. (**f**) Siliceous carbonaceous shale: the mineral composition is quartz, calcite, and organic matter. Q—quartz; Dol—dolomite; Cal—calcite; Bio—biotite; Mag—magnetite; Wit—witherite; OM—organic matter; Fsp—feldspar.

4.2. Mineral Content and Particle Size

The clastic minerals identified by using the TIMA were mainly quartz, feldspar, dolomite, calcite, biotite, muscovite, and hematite, which accounted for 67%–92% of the total mineral content. The clay mineral content in the rocks and soils in the Naore area was low, accounting for less than 1% of the total mineral content, and mainly consisted of chlorite and kaolinite. The organic matter content in the soil was high, accounting for about 13%–18% (Table 1). The specific mineral characteristics are described below.

Table 1. Mineral contents according to TIMA (%) and ATi–POS indexes in Naore village, Ziyang, southern Shaanxi, China.

	NR-08	**NR-13**	**NR-18**	**NRT-01**	**NRT-05**
	Carbonaceous Slate	**Siliceous Rock**	**Carbonaceous Shale**	**Soil**	**Soil**
Quartz	8.40	40.57	41.00	36.08	36.26
Albite	0.00	0.00	0.00	1.88	2.90
Plagioclase	0.03	0.09	0.61	1.45	1.23
Orthoclase	0.06	2.04	3.97	5.51	5.26
Calcite	8.72	0.04	0.16	0.24	0.33
Dolomite	71.09	0.00	13.57	1.74	0.60
Biotite	1.20	24.64	20.16	22.51	18.33
Muscovite	0.17	1.73	2.74	2.92	2.93
Chlorite-Clinochlore	0.76	0.00	0.31	0.21	0.06
Ankerite	1.04	0.00	0.32	0.03	0.02
Hematite	0.20	24.62	4.75	6.29	2.42
Pyrite	0.01	0.00	0.70	0.00	0.00
Schorl	0.00	0.01	0.06	0.08	0.14
Almandine-spessartine	0.00	3.82	0.58	2.86	4.92
Grossular	0.00	0.00	0.00	0.01	0.02
Pyrope	0.21	0.00	1.31	0.55	0.21
Kaersutite	0.01	0.08	0.59	0.60	0.73
Actinolite	0.00	0.07	0.02	0.06	0.96
Kinoshitalite	0.00	0.00	0.01	0.00	0.00
Ferro-Actinolite	0.07	0.24	0.82	0.19	0.17
Diopside	0.10	0.00	0.18	0.02	0.03
Allanite-(Ce)	0.00	0.00	0.02	0.00	0.01
Monazite	0.00	0.01	0.02	0.02	0.02
Titanite	0.00	0.04	1.17	0.09	0.60
Andradite	0.00	0.10	0.01	0.03	0.04
Apatite	1.31	0.81	1.72	1.65	1.60
Kaolinite	0.00	0.00	0.01	0.03	0.07
Olivine	0.56	0.00	1.43	0.41	0.15
Enstatite	0.00	0.00	0.06	0.01	0.15
Corundum	0.00	0.09	0.13	0.00	0.00
Xenotime-(Y)	0.00	0.00	0.00	0.02	0.00
Zircon	0.01	0.11	0.52	0.47	0.40
Ilmenite	0.00	0.05	0.01	0.10	0.12
Rutile	0.01	0.04	0.13	0.32	0.28
Goethite	0.00	0.03	0.00	0.05	0.02
Pyrrhotite	0.00	0.00	0.09	0.00	0.00

Table 1. *Cont.*

	NR-08	NR-13	NR-18	NRT-01	NRT-05
	Carbonaceous Slate	**Siliceous Rock**	**Carbonaceous Shale**	**Soil**	**Soil**
Romanechite	0.00	0.00	0.00	0.01	0.02
Zoisite	0.00	0.00	0.00	0.21	0.54
Alstonite	0.01	0.04	0.04	0.10	0.06
Total	93.98	99.32	97.25	86.76	81.63
POS	18.75	0.01	5.76	1.44	1.14
ATi	99.96	98.26	96.55	95.22	91.83

Notes: ATi = 100 × apatite/(apatite + tourmaline); POS = 100 × (pyroxene + olivine + spinel)/transparent heavy mineral.

4.2.1. Quartz

It is observed that quartz mainly exists in the form of cryptocrystalline polymers, veins, or clastic particles. A quartz vein exists in NR-08, and it is dense and crack-free. The surroundings of the quartz vein are corroded by calcite into irregular harbor shapes (Figure 4a,b), with a length of more than 14 mm. Cryptocrystalline quartz mainly exists in strips (Figure 4e,f), and the particle size is mainly concentrated in the range of 5–26 μm (Figure 5a). Biotite and other minerals are arranged in layers, and some are porphyritic. Quartz in the soil is mainly in the form of clastic particles with poor roundness and a very small size, with particles below 27 μm accounting for more than 97% of quartz (Figure 4g).

4.2.2. Carbonate Minerals

The carbonate minerals in the Naore area mainly include calcite and dolomite, which exist in the form of veins or polymers. Dolomite mainly exists in the form of aggregates (Figure 4b,c), in which there are a large number of cavities and cracks. It is the main component of the NR-08 sample, accounting for 79.8% of its total mineral content. Dolomite in other rock and soil samples appears in granular form (Figure 4f), with a particle size ranging from 5 to 25 μm (Figure 5b), bad idiomorphism, and content between 0.04% and 13.7%.

Calcite mainly exists in the form of colloidal quartz veins (Figure 4a), and a small amount of calcite exists in rock fractures in a granular shape. More calcite exists in dolomite cavities in the form of fine particles, with a particle size below 5 μm (Figure 4b,c). The calcite content of other samples is very low, and it exists in the form of fine particles. The particle size of calcite ranges from 5 to 26 μm (Figure 5b).

4.2.3. Biotite and Muscovite

The biotite in the Naore rock is mainly banded and interbedded with quartz (Figure 4e), symbiotic with orthoclase, and surrounded by hematite, and there are many muscovite alterations inside of it (Figure 4d). Biotite in the soil appears as dispersed particles with a particle size of about 10 μm. A small number of larger particles are amorphous and symbiotic with orthoclase and hematite (Figure 4g). The particle size of muscovite and biotite ranges from 3 to 18 μm (Figure 5c).

4.2.4. Feldspar

The feldspar (including plagioclase, albite, and orthoclase) content in the rock is relatively low, ranging from 0.09% to 4.59%. It is mainly orthoclase, which is sporadically distributed in biotite mineral particles (Figure 4d), with a particle size below 20 μm (Figure 5d). The feldspar content in the soil is slightly higher than that in the rock, which is between 8.8% and 9.4%, and it is also dominated by orthoclase, with small particles, only a few particles in the range of 50 μm, and most of them are symbiotic with biotite (Figure 4g).

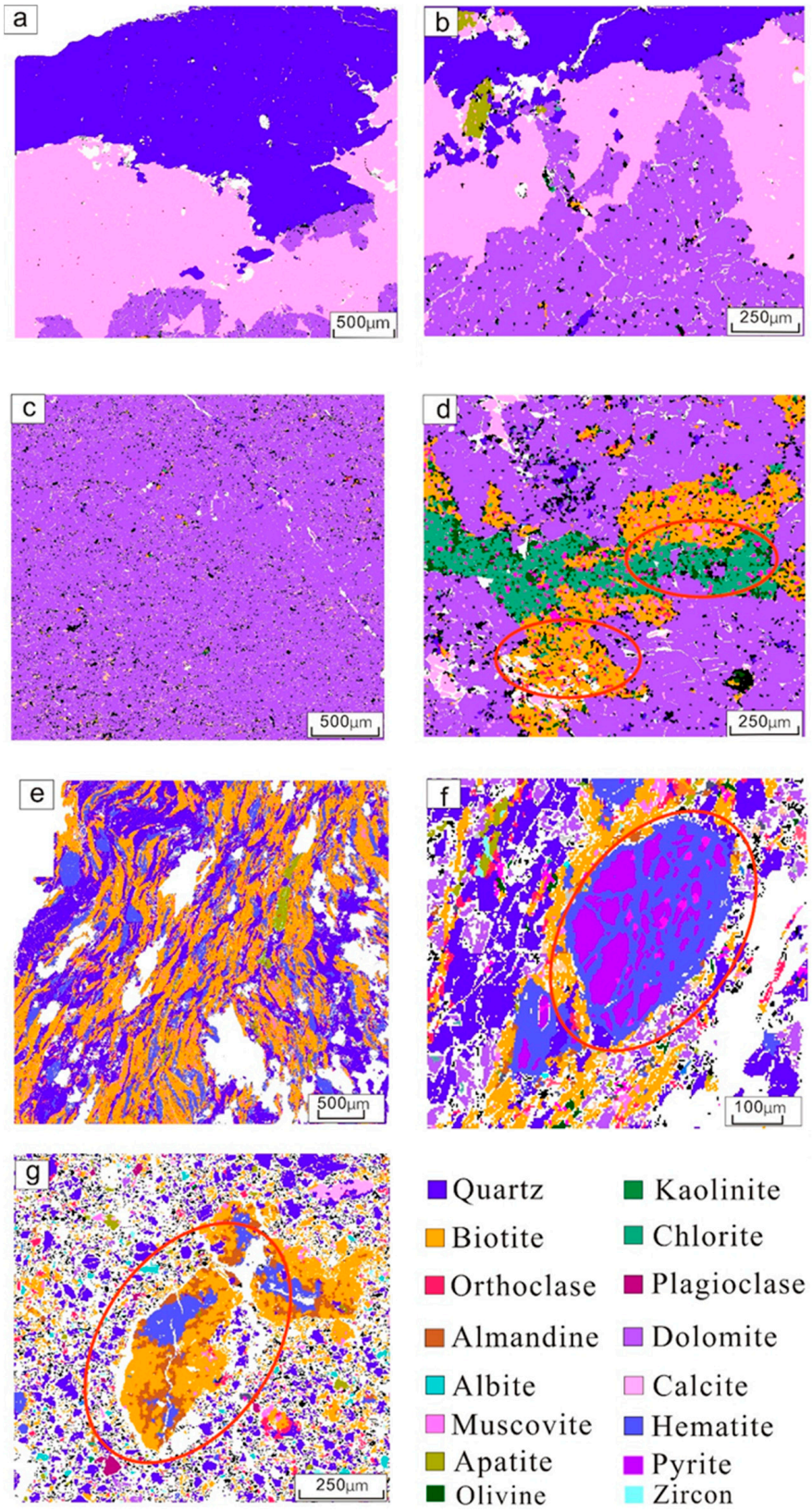

Figure 4. TIMA figures of mineral distribution in Naore village, Ziyang, southern China. (**a**) Quartz and calcite crisscross. (**b**) Calcite filled in dolomite as veins or fine particles. (**c**) Dolomite aggregate filled with calcite in the gap. (**d**) Biotite and chlorite growing in dolomite cracks. (**e**) Interbedding of biotite and quartz strips. (**f**) Hematite mainly in the form of alteration zones around pyrite. (**g**) Mineral distribution in soil.

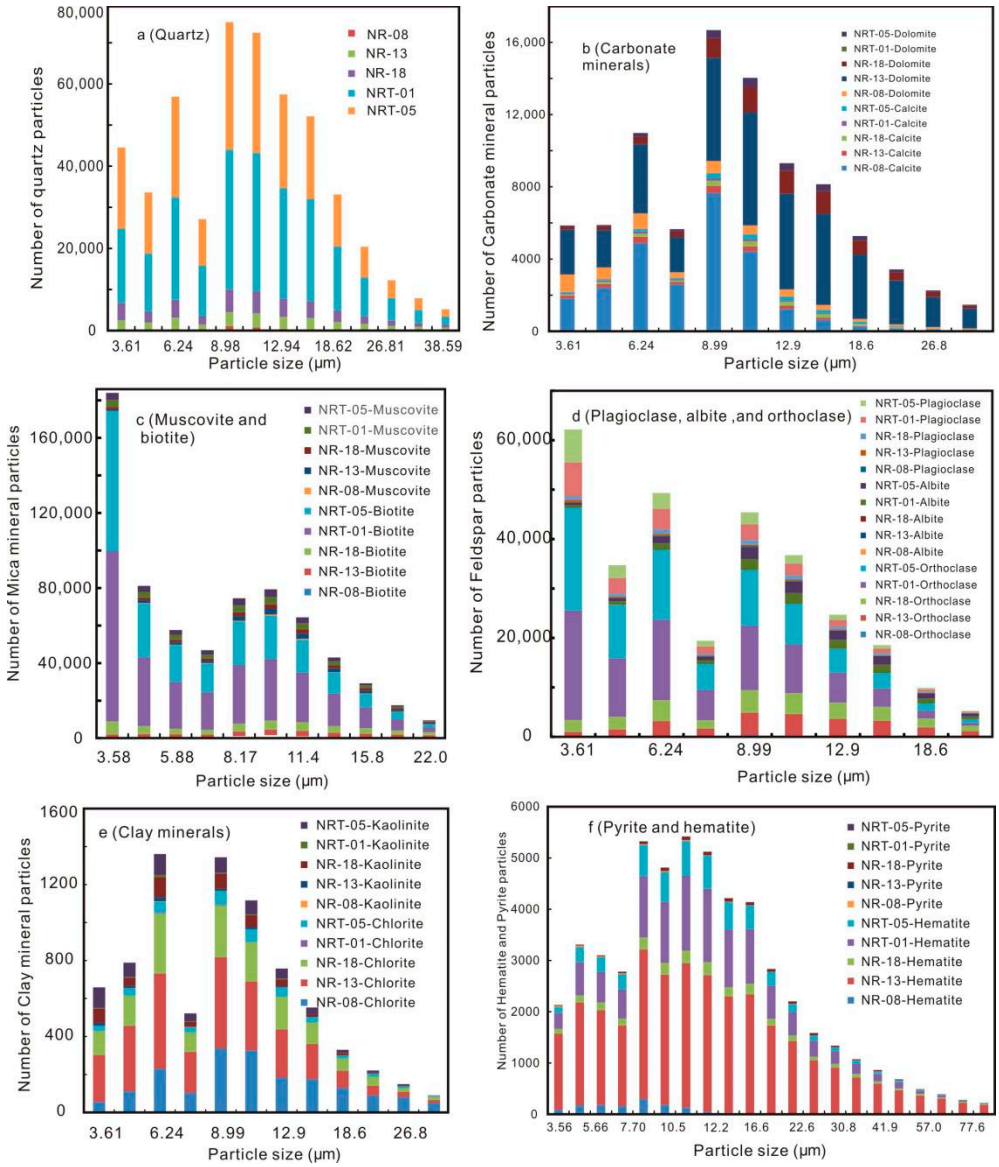

Figure 5. Distributions of different mineral grain sizes in Naore village, Ziyang, southern Shaanxi, China.

4.2.5. Clay Minerals

The content of clay minerals in this area is very low, accounting for only 0.001%–0.76% of the total mineral content. Chlorite is the main component, and the content of kaolinite is secondary. In the NR-08 sample, in which dolomite is the main component, chlorite exists in the dolomite gap in the form of aggregate and coexists with biotite (Figure 4d); in the other rock and soil samples, chlorite exists in the form of fine particles around biotite and feldspar, with a particle size ranging from 4 to 20 μm (Figure 5e).

4.2.6. Hematite

The content of hematite in the rocks and soils in this area is relatively high, accounting for 24.6% of the total minerals (NR-13). Hematite is mainly in the form of fine particles in rock strips or alteration zones around pyrite (Figure 4f), with particle sizes of 7–66 μm (Figure 5f). Hematite in the soil mostly exists in the form of independent minerals, with poor roundness and bad idiomorphism. There is often almandine symbiosis around them (Figure 4g).

4.2.7. Pyrite

Pyrite widely exists in the samples in the study area, but its growth is limited. Pyrite exists in the rock in the form of very fine grains. According to the data in Table 1, in NR-13, which has structural deformation, the content of pyrite is low, only sporadically appearing, while in NR-08, pyrite exists in the form of broken fine particles, with an average particle size of only 8.5 μm. The content of pyrite in NR-18 is relatively high, accounting for 0.7% of the total mineral content. Pyrite grows inside hematite, and the particle size is evenly distributed in the range of 5.81–55.7 μm (Figures 4f and 5f). There are few pyrite particles in the soil, and no obvious aggregation is formed. The pyrite in the study area is in the form of strawberry-like aggregates (from pyrite crystals with the size of several microns to tens of microns and aggregates of microcrystals).

4.2.8. Accessory Minerals

There are many kinds of accessory minerals in this area, but their contents are low. The accessory minerals account for 2.3% to 11.2% of the total mineral content, in which the content of almandine, olivine, zircon, and apatite is high, and that of other minerals is less than 1% (Table 1). Apatite is mainly distributed in rock crevices and is slightly idiomorphic (Figure 4b). Olivine and apatite are mainly distributed in the rock in the form of fine particles with a particle size below 50 μm, and they are also mostly distributed near the periphery of biotite. The accessory minerals are mostly very fine particles, with basically no grinding or self-shaping, and they are dispersed in rocks and soils.

4.3. Selenium Speciation

The contents of Se species in the black shales of Naore village in Ziyang, southern Shaanxi Province, varied greatly among the samples. The contents of the Se fraction were divided into two groups: A and B (Table 2). The order of the mass content of the five fractions of Se in Groups A and B were organically bound > Fe/Mn oxide bound > residual > exchangeable > carbonate bound and residual > exchangeable > organically bound > Fe/Mn oxide bound > carbonate bound, respectively.

Table 2. Distributions of selenium contents in various species in selenium-rich rocks and soils from Naore, Wamiao, and Guanquan in Ziyang, southern Shaanxi, China (mg/kg).

		Residual	Exchangeable	Carbonate Bound	Fe/Mn Oxide Bound	Organically Bound	Sum	Total Se
A	NR-1	0.86	0.21	<0.02	0.16	0.65	1.87	1.81
	NR-5	0.22	0.01	0.02	0.53	0.74	1.52	1.50
	NR-7	0.11	0.33	<0.02	0.02	0.56	1.02	0.83
	NR-8	0.88	0.08	<0.02	1.00	1.16	3.11	2.88
	NR-10	2.12	0.09	0.04	2.53	2.88	7.66	7.40
	Percent of speciation (%)	10.53~45.87	0.73~32.7	<3.00	1.95~34.92	34.52~54.76		
B	NR-3	18.55	0.48	0.48	0.36	1.83	21.70	18.82
	NR-13	23.47	0.81	<0.02	0.55	0.68	25.51	24.43
	NR-15	20.68	0.75	<0.02	0.22	0.45	22.11	21.66
	NR-17	15.92	0.73	<0.02	0.27	0.66	17.57	15.46
	NR-18	22.00	1.24	<0.02	0.27	1.08	24.60	23.58
	Percent of Se speciation (%)	85.52~93.55	3.19~5.04	<3.00	1.00~2.14	2.06~8.44		
Soil	NRT-01	19.10	0.46	<0.02	0.19	1.87	21.62	22.13
	NRT-03	18.80	0.45	<0.02	0.54	2.77	22.56	19.88
	NRT-05	14.02	0.44	0.03	0.27	2.50	17.25	17.12
	WMT-03	0.99	0.26	<0.02	0.16	1.98	3.40	3.15
	GQT-01	0.06	0.38	<0.02	0.22	1.56	2.22	1.78
	GQT-07	0.07	0.38	<0.02	0.11	1.33	1.88	1.56

In order to study and compare the quality of the Se fraction in the soil of the Ziyang area in Shaanxi, samples were collected from Naore, Wamiao, and Guanquan villages. The quality of the Se fraction in the samples from the three regions varied greatly. The order of the different fractions of Se in the soil of the three regions was as follows: (1) Naore: residual > organically bound > exchangeable > Fe/Mn oxide bound > carbonate bound; (2) Wamiao: organically bound > residual > exchangeable > Fe/Mn oxide bound > carbonate bound; (3) Guanquan: organically bound > exchangeable > residual > Fe/Mn oxide bound > carbonate bound (Table 2).

5. Discussion

5.1. Se Geochemical Enrichment Mechanism and Heavy-Mineral Sources

In the evolutionary history of the Earth, selenium has tended to be enriched in the mantle and core, with a lower content (~0.05 mg/kg) in normal sedimentary rocks [70]. Therefore, volcanic and post-magmatic hydrothermal processes are often considered an important source of selenium production [20,24]. Anomalous concentrations of Se, together with Cu, Pb, Zn, As, Sb, S, Ni, V, Mn, Mo, U, Ag, Au, and PGE, have been recognized in the Lower Cambrian 'black shales' in many parts of the Yangtze and Tarim cratons of southern and western China [7,8,16,18,19,24,62,71–76]).

At present, traces of hydrothermal activity have been found on mid-ocean ridges, in backarc basins, and in intracontinental rifts around the world [77]. The mediating effect of submarine hydrothermal microorganisms on mineral formation can affect local physical and chemical processes and result in the adsorption of various ions and minerals, playing an important role in mineral growth and precipitation [78]. Therefore, there is a certain connection between hydrothermal sedimentary diagenesis and selenium enrichment [77–79]. The extremely high Ba content in the samples suggests the influence of hydrothermal activity [61], and the hydrothermal source may be the rise in deep-sea heat source materials caused by strong submarine volcanic eruptions and intrusion activities along the deep fault [61,80,81]. In addition, black rock series-type deposits are distributed in NWW–SEE-trending rift basins and are consistent with the stratigraphic orientation. It can be inferred that the formation of a black rock series is closely related to faults, which may form small depressions with local enclosed anoxic conditions for the descending plates of different faults and which is conducive to the accumulation and evolution of organic matter [58,82]. In addition, the Se content in carbonaceous siliceous rocks and carbonaceous shale is higher than that in siliceous rocks, which may be related to the adsorption and protection effect of organic matter on the Se element [47,80,83]. In addition, the pores of clay minerals, quartz, pyrite, and other minerals play a certain adsorption role on elements, so the selenium content in samples rich in pyrite is significantly higher [21,46].

In the rock formations of the Ziyang area, the Lower Cambrian black shale is mainly composed of siliceous rocks, slate, shale, siliceous shale, and stone coal. In addition to being highly enriched in Ba, it is also rich in elements such as Se, Cu, V, and Cr, and it contains large amounts of layered pyrite, barite, witherite, and barium calcite [24,60,84]. During the weathering process, minerals decompose, and large amounts of Se, Ba, and V enter the soil. The Co, Mo, and W elements were significantly enriched in the soil of the sampling area, while Ag, Cd, V, Ba, Zn, As, Cu, Ni, U, Tl, and Sb also showed an enrichment trend [62]. The content of Mo, a typical mantle source element and an extremely enriched element in stone coal in the southern Shaanxi region, was 100 times higher in the interlayer of stone coal than in Chinese coal [85].

The composition of minerals in rocks is an important indicator for understanding the occurrence of trace elements. Selenium and sulfur belong to the same group of elements, with similar chemical properties, and selenium can replace sulfur in a similar form and enter sulfides, such as Fe (Se) S_2, Cu (Se) S, etc. [86–89]. There is a negative correlation between Se and both quartz and sodium feldspar in Ziyang rocks. As a weathering product of rock-forming minerals, illite is a clay mineral with a strong adsorption capacity for selenium, which can affect the migration behavior of selenium during rock weathering

through adsorption. In addition, there is a significant positive correlation between Se and pyrite content, which may indicate that pyrite is an important mechanism for selenium enrichment in rocks [52]. Clay minerals such as illite and chlorite usually have a strong adsorption capacity, and studies have also found that rocks, sediments, and soil all contain exchangeable selenium, that is, selenium adsorbed on the surface of clay minerals and iron manganese oxides [41,90,91]. Selenium tends to accumulate in weathered minerals such as biotite [88].

The characteristics of heavy minerals not only reflect the composition of the parent rock, but also reflect the physical separation, mechanical abrasion, and chemical dissolution of sediments in the sedimentation–transport and sedimentation processes [92]. The information inversion of the paleo sedimentary environment and paleotectonic activity by using the heavy-mineral characteristic index can show the tectonic activity stage and sedimentation characteristics, such as the material denudation and deposition rates [93]. The ATi index (100 × apatite/(apatite + tourmaline)) is used to determine the source of heavy minerals and the degree of heavy minerals' weathering [94]. The content POS (100 × (pyroxene + olivine + spinel)/transparent heavy mineral) of olivine, pyroxene, and spinel in heavy minerals can reflect the contribution of basic and ultrabasic rocks in the source area [95].

As shown in Table 1, the ATi and POS indexes of the research area were 91.83~99.96 and 0.01~18.75, respectively, reflecting the abundance of volcanic rock material in the source area. It has been shown that there are several intrusive rocks left over from magmatic activity in the Early Cambrian strata of Ziyang [60]. Selenium is more likely to undergo isomorphism with sulfur in high-temperature environments [96], and magmatic activity provides mantle-derived materials for diagenesis [24]. Research has found that there is a large-scale intrusion of diabase walls in the Ziyang area [97,98], and the selenium content in the strata is closely related to igneous rocks. Near igneous rocks (such as the diabase rocks in the Zhuwen River, Maobaguan), the mass fraction of selenium in carbon slate has reached 26.0 mg/kg [96]. There is a significant positive correlation between Se and V of the siliceous rock in Ziyang [52] and a positive correlation among Se, V, and P in the soil of the Daba Mountains in southern Shaanxi Province, which may indicate similarities in the genesis of Se-rich rock in western Hubei [99,100]. It was observed that the magmatic activity in the study area played a certain role in promoting the enrichment of selenium in the study area. In addition, the distribution of organic matter in black shale also increases the selenium content [53]. Under the same conditions, the Se content in stone coal can reach 41 mg/kg, which is higher than the content of the surrounding rock [96]. This is consistent with the results of previous research, that is, black shales in the Ziyang area are the result of the combined effects of hydrothermal sedimentation, volcanic activity, and biological processes [24,61,98,101].

5.2. The Relationship between Se Content and Speciation

By comparing the selenium content of the rocks in selenium-rich areas, it was found that rocks are greatly influenced by rock layers and lithology. Selenium is relatively rich in the rocks of the Upper Cretaceous strata in the United States [38], the Lower Permian Maokou Formation in Enshi [100,102,103], the Lower Cambrian Lujiaping Formation in Ziyang, and the Lower Cambrian Niutitang Formation in Zunyi [21,39,46]. Conversely, the selenium content is relatively low in the Silurian, Ordovician, Upper Middle Cambrian, and Lower Cambrian Jianzhuba Formations in Ziyang, southern Shaanxi, China [96,104]. Previous data have shown that the selenium content in stone coal in the selenium-rich area of Ziyang is the highest (average of 37.67 mg/kg), followed by slate, volcanic tuff, siliceous rock, mudstone, limestone, and dolomite. The selenium content of mudstone in the selenium-rich area of Enshi can reach up to 6084 mg/kg, followed by shale, siliceous rock, and stone coal, all of which have a content higher than 100 mg/kg. However, the selenium content of dolomite and limestone is relatively low, generally not exceeding 20 mg/kg [102]. The Ni-Mo deposit is generally rich in selenium in Zunyi, Guizhou, with

the highest selenium content in the Ni-Mo deposit (average of 1811 mg/kg), followed by montmorillonite, shale, phosphate rock, and siliceous rock [21,39]. The selenium content in the Upper Cretaceous selenium-rich rocks in South Dakota and Wyoming in the United States is relatively low, ranging from 0.42 to 70.7 mg/kg. Among them, the highest selenium content is in the Cretaceous rock, followed by siltstone and shale, and finally, montmorillonite [38].

The content of heavy-metal elements (V, Ni, and Zn) in black rock formations in the Ziyang area [62] is relatively low compared with that in the Yutangba area [105]. Compared to the black shales in the Longmaxi Formation of northern Yunnan Guizhou or western Newfoundland, the V content of the rocks in Ziyang is extremely high. The enrichment of elements is influenced by various factors in the soil. Studies have shown that the exposure of selenium-rich rocks is a necessary condition to accumulate high selenium content in a region's soil, and the main source of selenium or other heavy-metal elements in the soil is rocks [106,107]. Most areas that have reached selenium poisoning levels are often affected by human activities [106,108,109]. Human activities, especially mining, cultivation, and the use of black rock-rich coal, directly release elements from rocks into the surrounding soil [106,108]. For example, the use of stone coal in the Yutangba area has led to extremely high selenium content in some farmland areas [108], indicating the impact of human activities on the distribution of natural elements.

The highest reported selenium contents in carbonaceous shale, siliceous rock, and siliceous slate in the Ziyang area were 303 mg/kg [110], 278 mg/kg [24], and 128 mg/kg [52]. The average soil Se content in Ziyang County is 0.94 mg/kg, which is higher than the average soil Se content in China (0.29 mg/kg) [111] and Shaanxi Province (0.12 mg/kg) [112]. According to the classification criteria [113], most of soil Se belongs to the states of sufficient Se (35%) and rich Se (42%) [114]. From Table 2, we can see that the Se content in the rock and soil is classified as rich Se, and the soil Se concentrations are controlled by the parent rock and organic matter [52].

Se speciation in rock is dependent on the rock's content and morphology. Therefore, the selenium content and its morphological characteristics in the soil are significantly correlated with the distribution of selenium species in the rocks in the Ziyang area [52]. Selenium mainly exists in the form of hydrophilic organic compounds in rocks and soil. It is generally believed that soluble selenium has the highest bioavailability, followed by exchangeable selenium [115]. Selenium combined with Fe-Mn is difficult for plants to utilize [116]. The binding of selenium into its organic form in rocks and soil limits its migration ability and effectiveness for plants [117], while the residual form is the most stable in rocks and soil [52]. When the pH of the environment decreases, these species of selenium are preferentially separated, leading to an increase in the bioavailable selenium content in the soil [118]. Acidic environments are not conducive to the dissociation of other bound forms of selenium in the soil. On the contrary, selenium-rich soil is alkaline, and the various selenium-binding states tend to decompose and release free selenium, enhancing the bioavailability of selenium. Therefore, the pH value of the regional environment plays an important role in controlling the effective selenium content in the soil and the plant absorption capacity [118].

The effective selenium content in Ziyang's selenium-rich rocks is not higher than 10% (5.42 $\pm$ 3.40%), and most of the rocks (except for stone coal and limestone) have a Se content between 4.55% and 6.77%. The effective selenium content in carbonaceous shale in the Enshi area accounts for 6.32%–24.35% of the total selenium content, with an average of 17.81 $\pm$ 6.80%. The content is mostly around 20%, which is much higher than the effective selenium ratio in Ziyang selenium-rich carbonaceous shale and carbonaceous siliceous rock but lower than the effective selenium ratios of 21.51% and 24.36% in the Lower Cambrian black shale and carbonaceous siliceous rock in Zunyi, China [39,52]. There are certain differences in the main occurrence states of selenium in rocks from the two major selenium-rich areas in China: (1) In Ziyang, southern Shaanxi Province, the sulfur-/selenide-bound, organically bound, and residual forms are the main species in carbonaceous slate [52],

which is consistent with the results of this study (Table 3). (2) In Enshi, western Hubei Province, the organically bound, sulfur-/selenide-bound, and exchangeable forms are the main species in carbonaceous shale [39].

Table 3. The percentage contents of different Se species in selenium-rich rocks and soils from different areas.

	Residual	Exchangeable	Carbonate Bound	Fe/Mn Oxide Bound	Organically Bound	Water Soluble	Humic Acid Bound
NRT-01	88.32%	2.15%	0.09%	0.86%	8.66%	~	~
NRT-03	83.34%	1.98%	0.09%	2.40%	12.28%	~	~
NRT-05	81.28%	2.53%	0.15%	1.57%	14.48%	~	~
WMT-03	29.19%	7.74%	0.90%	4.83%	58.24%	~	~
GQT-01	2.92%	16.93%	1.06%	9.75%	70.41%	~	~
GQT-07	3.50%	20.06%	1.06%	5.78%	70.66%	~	~
Mingbei [119]	34.85%	9.25%		7.50%	46.56%	1.84%	~
Shandong [120]	34.82%	1.54%	3.20%	0.17%	38.22%	1.00%	21.95%
Ningxia [121]	50.11%	5.32%	2.55%	2.40%	23.01%	5.43%	11.18%
Qinghai [122]	42.95%	3.06%	3.06%	1.47%	31.83%	3.32%	14.31%
Anhui [123]	26.69%	7.50%	4.19%	2.75%	38.46%	2.05%	18.36%
Inner Mongolia [124]	29.63%	5.51%	3.32%	1.60%	18.54%	3.24%	23.41%

By comparing it with other selenium-rich soil (tea gardens in northern Fujian Province [119], the selenium-rich areas in Qingzhou City—Shandong Province [120], northern Ningxia Province [121], Lujiang—Anhui Province [123], eastern Qinghai Province [122], and Bayannur—Inner Mongolia [124]), it was determined that the selenium-rich soil is mainly composed of the organically bound and residual species, accounting for 23.01% to 46.56% and 26.69% to 50.11%, respectively (Table 3). The second main species is humic-acid-bound, accounting for 23.41% in Inner Mongolia. The proportion of exchangeable, carbonate-bound, Fe-Mn oxide-bound, and water-soluble forms in each selenium-rich region is relatively small. Through a comprehensive comparison, it was found that the proportions of different species of selenium in various selenium-rich regions are in the following order: organic/residual > humic acid bound > water soluble/exchangeable/carbonate bound > Fe-Mn oxide bound. By comparing the results of this study with those of previous studies (Table 3), it was found that there is a high degree of consistency in the distribution of selenium species between the area examined in this study and other selenium-rich regions. In addition, the Se content is directly proportional to the organic/residual species.

6. Conclusions

We conducted a systematic study of Se mineralogy and speciation in the Lower Cambrian Se-enriched strata within the Lujiaping Formation in southern Shaanxi Province, China, to examine the Se geochemical enrichment mechanism and the relationship between the Se content and its species. In the rock formations of the Ziyang area, the Lower Cambrian black shale is mainly composed of siliceous rocks, slate, shale, siliceous shale, and stone coal. The minerals in Naore village, Ziyang, Shaanxi Province, include quartz, carbonate minerals (calcite and dolomite), feldspar (plagioclase, albite, and orthoclase), biotite and muscovite, clay minerals (chlorite and kaolinite), hematite, pyrite, and accessory minerals (almandine, olivine, zircon, and apatite). A negative correlation was observed between Se and both quartz and sodium feldspar. In addition, selenium tended to accumulate in clay minerals such as illite and chlorite and in weathered minerals such as biotite. The ATi and POS indexes of heavy minerals in the research area were 91.83~99.96 and 0.01~18.75, respectively, reflecting the abundance of volcanic rock material in its source. Black shales in the Ziyang area are the result of the combined effects of hydrothermal sedimentation, volcanic activity, and biological processes. The Se content in the rock and soil of the study area is classified as rich Se, and the soil Se concentrations are controlled by the parent rock and organic matter. The fraction of selenium in various selenium-rich areas

is mainly present as unusable residues and organic forms, followed by humic-acid-bound selenium. The proportions of water-soluble, exchangeable, and carbonate-bound selenium are relatively small, and the proportion of Fe-Mn oxide-bound selenium is the lowest.

Author Contributions: Conceptualization, C.F. and S.L.; methodology, W.S.; software, C.H.; validation, S.L.; formal analysis, W.S.; investigation, C.F. and C.H.; resources, S.L.; data curation, Y.Y.; writing—original draft preparation, C.F.; writing—review and editing, S.L.; visualization, Y.Y.; supervision, S.L.; project administration, C.F.; funding acquisition, S.L. All authors have read and agreed to the published version of the manuscript.

Funding: This research was funded by the Major Research Plan of National Natural Science Foundation of China, grant No. 92062219 and the Key Project of Natural Science Basic Research Program of Shaanxi Province, grant No. 2023-JC-ZD-16.

Data Availability Statement: Data will be made available upon request.

Acknowledgments: We thank three anonymous reviewers for improving the manuscript.

Conflicts of Interest: The authors declare that they have no known competing financial interests or personal relationships that could have appeared to influence the work reported in this paper.

References

1. Jaffe, L.A.; Peucker, E.B.; Petsch, S.T. Mobility of rhenium, platinum group elements and organic carbon during black shale weathering. *Earth Planet. Sci. Lett.* **2002**, *198*, 339–353. [CrossRef]
2. Lipinski, M.; Warning, B.; Brumsack, H.J. Trace metal signatures of Jurassic/Cretaceous black shales from the Norwegian shelf and the Barents Sea. *Palaeogeogr. Palaeoclimatol. Palaeoecol.* **2003**, *190*, 459–475. [CrossRef]
3. Piper, D.Z.; Calvert, S.E. A marine biogeochemical perspective on black shale deposition. *Earth Sci. Rev.* **2009**, *95*, 63–96. [CrossRef]
4. Anjum, F.; Bhatti, H.N.; Asgher, M.; Shahid, M. Leaching of metal ions from black shale by organic acids produced by *Aspergillus niger*. *Appl. Clay Sci.* **2010**, *47*, 356–361. [CrossRef]
5. Baioumy, H.; Ulfa, Y.; Nawawi, M.; Padmanabhan, E.; Anuar, M.N.A. Mineralogy and geochemistry of Palaeozoic black shales from Peninsular Malaysia: Implications for their origin and maturation. *Int. J. Coal Geol.* **2016**, *165*, 90–105. [CrossRef]
6. Yan, D.T.; Li, S.J.; Fu, H.J.; Jasper, D.M.; Zhou, S.D.; Yang, X.R.; Zhang, B.; Mangi, H.N. Mineralogy and geochemistry of lower Silurian black shales from the Yangtze platform, South China. *Int. J. Coal Geol.* **2021**, *237*, 103706. [CrossRef]
7. Jiang, S.Y.; Yang, J.H.; Ling, H.F.; Chen, Y.Q.; Feng, H.Z.; Zhao, K.D.; Ni, P. Extreme enrichment of polymetallic Ni-Mo-PGE-Au in Lower Cambrian black shales of South China: An Os isotope and PGE geochemical investigation. *Palaeogeogr. Palaeoclimatol. Palaeoecol.* **2007**, *251*, 217–228. [CrossRef]
8. Fan, D.L.; Yang, R.D.; Huang, Z.X. The Lower Cambrian black shale series and iridium anomaly in South China. In Proceedings of the Development in Geoscience, Contributions to the 27th International Geological Congress, Moscow, Russia, 4–14 August 1984; Science Press: Beijing, China, 1984; pp. 215–224.
9. Yang, J.H.; Jiang, S.Y.; Ling, H.F.; Chen, Y.Q. Re-Os isotope tracing and dating of black shales and oceanic anoxic events. *Earth Sci. Front.* **2005**, *12*, 243–250.
10. Hsu, K.J.; Oberhänsli, H.; Gao, J.Y.; Sun, S.; Chen, H.D.; Krähenbühl, U. Strangelove ocean before the Cambrian explosion. *Nature* **1985**, *316*, 809–811. [CrossRef]
11. Orberger, B.; Pasava, J.; Gallien, J.P.; Daudin, L.; Trocellier, P. Se, As, Mo, Ag, Cd, In, Sb, Pt, Au, Tl, Re traces in biogenic and abiogenic sulfides from Black Shales (Selwyn Basin, Yukon territories, Canada): A nuclear microprobe study. *Nucl. Instrum. Methods Phys. Res. Sect. B* **2003**, *210*, 441–448. [CrossRef]
12. Hu, Y.H.; Sun, W.D.; Ding, X.; Wang, F.Y.; Ling, M.X.; Liu, J. Volcanic event at the Ordovician-Silurian boundary: The message from K-bentonite of Yangtze Block. *Acta Petrol. Sin.* **2009**, *25*, 3298–3308.
13. Jiang, Y.H.; Yue, W.Z.; Ye, Z.Z. Characteristics, sedimentary environment and origin of the Lower Cambrian stone-like coal in southern China. *Coal Geol. China* **1994**, *6*, 26–31. (In Chinese with English Abstract)
14. Su, W.B.; Li, Z.M.; Ettensohn, F.R.; Johnson, M.E.; Huff, W.D.; Wang, W.; Ma, C.; Li, L.; Zhang, L.; Zhao, H.J. Distribution of Black Shale in the Wufeng-Longmaxi Formations (Ordovician-Silurian), South China: Major Controlling Factors and Implications. *Earth Sci.* **2007**, *32*, 819–827. (In Chinese with English Abstract) [CrossRef]
15. Li, H.B. Comparative Analysis of Shale Gas Reservoir Between the Marine Shale Gas in the Southern Shaanxi and the Terrestrial Shale Gas in the Northern Shaanxi Province. *Geol. Shaanxi* **2018**, *36*, 34–37. (In Chinese with English Abstract)
16. Chen, N.S. Lower Cambrian black shale series and associated stratiform deposits in southwest China. *Chin. J. Geochem.* **1990**, *9*, 244–255. [CrossRef]
17. Pasava, J.; Hladikova, J.; Dobes, P. Origin of Proterozoic metal-rich black shales from the Bohemian Massif, Czech Republic. *Econ. Geol.* **1996**, *91*, 63–79. [CrossRef]

18. Steiner, M.; Wallis, E.; Erdtmann, B.D.; Zhao, Y.L.; Yang, R.D. Submarine-hydrothermal exhalative ore layers in black shales from South China and associated fossils-insights into a Lower Cambrian facies and bio-evolution. *Palaeogeogr. Palaeoclimatol. Palaeoecol.* **2001**, *169*, 165–191. [CrossRef]
19. Orberger, B.; Vymazalova, A.; Wagner, C.; Fialin, M.; Gallien, J.P.; Wirth, R.; Pasava, J.; Montagnac, G. Biogenic origin of intergrown Mo-sulphide-and carbonaceous matter in Lower Cambrian black shales (Zunyi Formation, Southern China). *Chem. Geol.* **2007**, *238*, 213–231. [CrossRef]
20. Feng, C.X.; Liu, S.; Coulson, I.M. Lithological and Si-O-S isotope geochemistry: Constraints on the origin and genetic environment of the selenium (Se)-rich siliceous rocks in Enshi, Hubei Province, China. *Acta Geochim.* **2021**, *40*, 89–105. [CrossRef]
21. Feng, C.X.; Liu, S.; Hu, R.Z.; Chi, G.X. Geochemistry of the lower Cambrian selenium-rich black rock series in Zunyi: Genesis and selenium enrichment mechanism. *Earth Sci. J. China Univ. Geosci.* **2010**, *35*, 947–958. (In Chinese with English Abstract) [CrossRef]
22. Awan, R.S.; Liu, C.L.; Khan, A.; Zang, Q.B.; Wu, Y.P.; Feng, D.H. Sedimentary geochemistry of the Early Cambrian Niutingtang Formation to reconstruct the palaeo-depositonal environments and to evaluate the organic matter enrichment mechanism from the Yangtze Block, South China. *Geol. J.* **2022**, *57*, 380–409. [CrossRef]
23. Luo, K.L.; Xu, L.R.; Tan, J.A.; Wang, D.H. Selenium source in the selenosis area of the Daba region, South Qinling Mountain, China. *Environ. Earth Sci.* **2004**, *45*, 426–432. [CrossRef]
24. Feng, C.X.; Chi, G.X.; Liu, J.J.; Hu, R.Z.; Liu, S.; Ian, M.C. Geochemical constraints on the origin and environment of lower Cambrian, selenium-rich siliceous sedimentary rocks in the Ziyang area, Daba region, central China. *Int. Geol. Rev.* **2012**, *54*, 765–778. [CrossRef]
25. Liu, J.J.; Zheng, M.H.; Liu, J.M.; Su, W.C. Geochemistry of the La'erma and Qiongmo Au-Se deposits in western Qinling Mountains, China. *Ore Geol. Rev.* **2000**, *17*, 91–111. [CrossRef]
26. Song, C.Z. A brief description of the Yutangba sedimentary-type selenium mineralized area in southwestern Hubei. *Miner. Depos.* **1989**, *8*, 83–89. (In Chinese with English Abstract)
27. Wang, H.F.; Li, J.Q. The geological characteristic of Se-deposit in Shuanghe, Enshi, Hubei Province. *Hubei Geol.* **1996**, *10*, 10–21. (In Chinese with English Abstract)
28. Thompson, M.; Rouch, C.; Braddock, W. New occurence of native selenium. *Am. Mineral.* **1956**, *41*, 156–157.
29. Coleman, R.G.; DeleVaux, M.H. Occurrence of selenium in sulfides from some sedimentary rocks of the United States. *Econ. Geol.* **1956**, *51*, 112. [CrossRef]
30. Yi, S.T.; Li, B.H.; Xue, X.T. Mineraligy of Natural Selenium In Yamadu Region, Ili River. *Xinjiang Geol.* **1988**, *6*, 12–15. (In Chinese with English Abstract)
31. Chen, L.M.; Li, D.R.; Wang, G.X.; Zhang, Q.F. Antimonselite—A New Mineral. *Acta Mineral. Sin.* **1993**, *13*, 7–11. (In Chinese with English Abstract) [CrossRef]
32. Zheng, M.H.; Liu, J.J.; Liu, J.M.; Lu, W.Q. The First Discovery and Preliminary study of Selenio-Sulfantimonide in China. *Mineral. Petrol.* **1993**, *13*, 9–13. (In Chinese with English Abstract)
33. Yao, L.B.; Gao, Z.M.; Yang, Z.S.; Long, H.B.; Ye, X.X.; Wang, M.Z. A Study on the Existing Forms of Selenium in Yutangba Independent Selenium Deposit by Electron-Microprobe Analysis. *Acta Mineral. Sin.* **2001**, *21*, 49–52. (In Chinese with English Abstract)
34. Wen, H.J. *Mineralogy, Geochemistry and Metallogenic Mechanism of Selenium-Take Laerma Selenium-Gold Deposit and Some Selenium Bearing Formations as Example*; Institute of Geochemistry, Chinese Academy of Sciences: Guiyang, China, 1999. (In Chinese with English Abstract)
35. Jia, B.; Xian, C.G.; Tsau, J.S.; Zuo, X.; Jia, W.F. Status and Outlook of Oil Field Chemistry-Assisted Analysis during the Energy Transition Period. *Energy Fuels* **2022**, *36*, 12917–12945. [CrossRef]
36. Zhang, Y.Q.; Moore, J.N. Selenium fractionation and speciation in a wetland system. *Environ. Sci. Technol.* **1996**, *30*, 2613–2619. [CrossRef]
37. Zhang, Y.Q.; Moore, J.N.; Frankenberger, W.T. Speciation of soluble selenium in agricultural drainage waters and aqueous soil-sediment extracts using hydride generation atomic absorption spectrometry. *Environ. Sci. Technol.* **1999**, *33*, 1652–1656. [CrossRef]
38. Kulp, T.R.; Pratt, L.M. Speciation and weathering of selenium in upper cretaceous chalk and shale from South Dakota and Wyoming, USA. *Geochim. Cosmochim. Acta* **2004**, *68*, 3687–3701. [CrossRef]
39. Fan, H.F.; Wen, H.J.; Hu, R.Z.; Zhao, H. Selenium speciation in Lower Cambrian Se-enriched strata in South China and its geological implications. *Geochim. Cosmochim. Acta* **2011**, *75*, 7725–7740. [CrossRef]
40. Zhang, Z.; Zhou, L.Q.; Zhang, Q. Speciation of Selenium in Geochemical Samples by Partial Dissolution Technique. *Rock Miner. Anal.* **1997**, *4*, 255–261. (In Chinese with English Abstract)
41. Martens, D.A.; Suarez, D.L. Selenium Speciation of Soil/Sediment Determined with Sequential Extractions and Hydride Generation Atomic Absorption Spectrophotometry. *Environ. Sci. Technol.* **1997**, *31*, 133–139. [CrossRef]
42. Plant, J.A.; Kinniburgh, D.G.; Smedley, P.L.; Fordyce, F.; Klinck, B. 9.02–Arsenic and Selenium. *Treatise Geochem.* **2003**, *9*, 17–66.
43. Mei, Z.Q. Summary on two selenium-rich areas of China. *Chin. J. Endem.* **1985**, *4*, 379–385. (In Chinese with English Abstract)
44. Tian, H.; Ma, Z.Z.; Chen, X.L.; Zhang, H.Y.; Bao, Z.Y.; Wei, C.H.; Xie, S.Y.; Wu, S.T. Geochemical Characteristics of Selenium and Its Correlation to Other Elements and Minerals in Selenium-Enriched Rocks in Ziyang County, Shaanxi Province, China. *J. Earth Sci.* **2016**, *27*, 763–776. (In Chinese with English Abstract) [CrossRef]

45. Liu, J.J.; Zheng, M.H.; Liu, J.M.; Zhou, Y.F.; Gu, X.X.; Zhang, B. The geological and geochemical characteristics of Cambrian chert and their sedimentary environmental implications in western Qinling. *Acta Petrol. Sin.* **1999**, *15*, 145–154. (In Chinese with English Abstract)
46. Luo, K.L.; Pan, Y.T.; Wang, W.Y.; Tan, J.A. Selenium contents and distribution patterns in the Palaeozoic strata in Southern Qinling Mountains. *Geol. Rev.* **2001**, *47*, 211–217. (In Chinese with English Abstract) [CrossRef]
47. Luo, K.L. The Lujiaping Formation of northern Daba Mountain. *J. Stratigr.* **2006**, *30*, 149–156. (In Chinese with English Abstract)
48. Luo, K.L.; Qiu, X.P. Analysis on selenium-rich crops in Ankang district, Shaanxi—The case of Ziyang County. *Nat. Resour.* **1995**, *2*, 68–72. (In Chinese with English Abstract)
49. Zhao, C.Y.; Ren, J.H.; Xue, C.Z. Selenium of soil in rich selenium area-Ziyang. *Acta Pedol. Sin.* **1993**, *30*, 253–259. (In Chinese with English Abstract)
50. Wang, L.S. Study on the Metallogenic Regularity and Geological-Geochemistry for Black Rock Seriesand Related Typical Deposits in Qinling Mounitains, Shaanxi. Ph.D. Thesis, Northwest University, Xi'an, China, 2009. (In Chinese with English Abstract)
51. Gao, X.H. On the poly metal elements occurrence of black rock seris in Zhenping Region of south Qinling-north Dabashan. *Value Eng.* **2015**, *20*, 176–177. (In Chinese with English Abstract) [CrossRef]
52. Tian, H. *The Occurrence State and Speciation of Selenium and Its Environmental Behaviors in Rock-Soil-Plant from Typical High-Se Area*; A Dissertation Submitted to China University of Geosciences; China University of Geosciences(Wuhan): Wuhan, China, 2017. (In Chinese with English Abstract)
53. Zhao, H.B.; Feng, C.X.; Liu, S.; Liu, F.X. Organic geochemical characteristics of lower Cambrian black rock series in Ziyang, Shaanxi Province. *J. Jilin Univ. Earth Sci. Ed.* **2023**, *53*, 1016–1032. (In Chinese with English Abstract) [CrossRef]
54. Chen, Q.; Song, W.L.; Yang, J.K.; Hu, Y.; Huang, J.; Zhang, T.; Zhen, G.S. Principle of automated mineral quantitative analysis system and its application in petrology and mineralogy: An example from TESCANTIMA. *Miner. Depos.* **2021**, *40*, 345–368. (In Chinese with English Abstract) [CrossRef]
55. Fan, D.L.; Ye, J.; Yang, R.Y.; Huang, Z.X. The Geological Events and Ore Mineralization Nearby the Precambrian-Cambrian Boundary in Yangtze Platform. *Acta Sedimentol. Sin.* **1987**, *5*, 81–95. (In Chinese with English Abstract)
56. Zhang, G.W.; Zhang, B.R.; Yuan, X.C. *Qinling Orogenic Belt and Continental Dynamics*; Science Press: Beijing, China, 2001; pp. 1–855. (In Chinese)
57. He, J.K.; Lu, H.X.; Zhu, B. The Tectonic Inversion and Its Geodynamic Processes in Northern Daba Mountains of Eastern Qinling Orogenic Belt. *Sci. Geol. Sin. Chin. J. Geol.* **1999**, *32*, 14–28. (In Chinese with English Abstract)
58. Xie, H. *Organic Geochemistry and Ore-Forming Environment of the Large Witherite Deposits in Northern Daba Mountains, China*; China University of Geosciences: Beijing, China, 2006. (In Chinese with English Abstract)
59. Luo, K.L. The age of rock distribution in the selenosis region, south Shaanxi Province. *Geol. Rev.* **2003**, *49*, 383–388. (In Chinese with English Abstract)
60. Shaanxi Bureau of Geology and Mineral Resources. *Regional Geology of Shaanxi Province*; Geological Publishing House: Beijing, China, 1989. (In Chinese)
61. Wang, S.X.; Feng, C.C.; Liu, S.; Fan, Y. Geochemistry of the lower Cambrian black rock series in Ziyang, Shaanxi Province: Geochemical characteristics and petrogenesis. *Acta Sedimentol. Sin.* **2020**, *38*, 980–993. (In Chinese with English Abstract) [CrossRef]
62. Hou, C.H.; Feng, C.X.; Liu, S.; Zhao, H.B. Distribution and pollution assessment of selenium and heavy metals in soil: Ziyang, Shaanxi Province as an example. *J. Northwest Univ. Nat. Sci. Ed.* **2022**, *52*, 878–890. (In Chinese with English Abstract) [CrossRef]
63. Cui, Y.Y.; Zhou, Y.L.; Chen, G.X.; Huang, C.C.; Pang, J.L.; Yang, J.M.; Yan, X.J. Mineral quantitative analysis of Mu Us sandy land with QEMSCAN. *Arid. Land Geogr.* **2020**, *43*, 1505–1513. (In Chinese with English Abstract) [CrossRef]
64. Zhang, H.Z.; Lu, H.Y.; Zhou, Y.L.; Cui, Y.Y.; Zhang, J.; Lv, F.; Chen, Y.Z. Quantitative analysis of the clastic mineral composition in sediments from the Weihe River Basin by scanning electron microscope and its implication for provenance. *Acta Sedimentol. Sin.* **2022**, *40*, 944–956. (In Chinese with English Abstract) [CrossRef]
65. Fan, H.F.; Wen, H.J.; Ling, H.W.; Yu, W.X. Determination of trace selenium in geological samples by Hydride generation atomic fluorescence spectrometry-a comparative experiment of two different dissolution methods. *Bull. Mineral. Petrol. Geochem.* **2005**, *24*, 200–203. (In Chinese with English Abstract)
66. Tessier, A.; Campbell, P.G.C.; Bisson, M. Sequential extraction procedure for the speciation of particulate trace metals. *Anal. Chem.* **1979**, *51*, 844–851. [CrossRef]
67. Qu, J.G.; Xu, B.X.; Gong, S.C. Selenium speciation of soil/sediment determined with sequential extractions scheme. *Environ. Chem.* **1997**, *16*, 277–283.
68. Loucks, R.G.; Reed, R.M.; Ruppel, S.C.; Hammes, U. Spectrum of pore types and networks in mudrocks and a descriptive classification for matrix-related mudrock pores. *AAPG Bull.* **2012**, *96*, 1071–1098. [CrossRef]
69. Wang, X.P.; Mou, C.L.; Ge, X.Y.; Chen, X.W.; Zhou, K.K.; Wang, Q.Y.; Liang, W. Mineral component characteristics and evaluation of black rock series of Longmaxi Formation in southern Sichuan and its periphery. *Acta Pet. Sin.* **2015**, *36*, 150–162. (In Chinese with English Abstract) [CrossRef]
70. Liu, Y.J.; Cao, L.M.; Li, Z.L.; Wang, H.N.; Chu, T.Q.; Zhang, J.R. *Element Geochemistry*; Science Press: Beijing, China, 1984; pp. 1–281. (In Chinese)

71. Fan, D.L. Polyelements in the Lower Cambrian black shale series in southern China. In *The Significance of Trace Metals in Solving Petrogenetic Problems and Controversies*; Augustithis, S.S., Ed.; The Ophrastus Publication: Athens, Greece, 1983; pp. 447–474.
72. Li, S.R.; Gao, Z.M. Silicalites of hydrothermal origin in the Lower Cambrian black rock series of South China. *Chin. J. Geochem.* **1996**, *15*, 113–120. [CrossRef]
73. Li, S.R.; Gao, Z.M. Source tracing of noble metal elements in Lower Cambrian black rock series of Guizhou Hunan Province, China. *Sci. China (Ser. D Earth Sci.)* **2000**, *43*, 625–632. [CrossRef]
74. Mao, J.W.; Bernd, L.; Du, A.D.; Zhang, G.D.; Ma, D.S.; Wang, Y.T.; Zeng, M.G.; Robert, K. Re-Os Dating of Polymetallic Ni-Mo-PGE-Au Mineralization in Lower Cambrian Black Shales of South China and Its Geologic Significance. *Econ. Geol.* **2002**, *97*, 1051–1061. [CrossRef]
75. Jiang, S.Y.; Yang, J.H.; Ling, H.F.; Feng, H.Z.; Chen, Y.Q.; Chen, J.H. Re-Os isoptopes and PGE geochemistry of black shales and intercalated Ni-Mo polymetallic sulfide bed from the Lower Cambrian Niutitang Formation, South China. *Prog. Nat. Sci.* **2003**, *13*, 788–794. [CrossRef]
76. Jiang, S.Y.; Chen, Y.Q.; Ling, H.F.; Yang, J.H.; Feng, H.Z.; Ni, P. Trace and rare-earth element geochemistry and Pb-Pb dating of black shales and intercalated Ni-Mo-PGEAu sulfide ores in Lower Cambrian strata, Yangtze Platform, South China. *Miner. Depos.* **2006**, *41*, 453–467. [CrossRef]
77. Li, J.H.; Chu, F.Y.; Feng, J. Advances in deep-sea hydrothermal microbial mineralisation and the deep biosphere. *Prog. Nat. Sci.* **2005**, *15*, 1416–1425. (In Chinese with English Abstract)
78. Qiu, X.; Wang, H.M.; Liu, D.; Gong, L.F.; Wu, X.P.; Xiang, X. The physiological response of synechococcus elongatus to salinity: A potential biomarker for ancient salinity in evaporative environments. *Geomicrobiol. J.* **2012**, *29*, 477–483. [CrossRef]
79. Han, S.C.; Hu, K.; Cao, J. Organic geochemistry of barite deposits hosted in the Early Cambrian black shales from the Tianzhu County, Guizhou Province. *Geochimica* **2014**, *43*, 386–398. (In Chinese with English Abstract) [CrossRef]
80. Liu, J.J.; Zhai, D.G.; Wang, D.Z.; Gao, S.; Yin, C.; Liu, Z.J.; Wang, J.P.; Wang, Y.H.; Zhang, F.F. Classification and mineralization of the Aur-(Ag)-Te-Se deposits. *Earth Sci. Front.* **2020**, *27*, 79–98. (In Chinese with English Abstract) [CrossRef]
81. Yang, J.; Yi, F.C. A Study on Occurrence Modes and Enrichment Patterns of Lower Cambrian Black Shale Series in Northern Guizhou Province, China. *Acta Mineral. Sin.* **2012**, *32*, 281–287. (In Chinese with English Abstract) [CrossRef]
82. Wen, H.J.; Zhou, Z.B.; Ma, W.P.; Zhu, Y. Research progresses and main scientific issues of strategically critical minerals in black rock series. *Bull. Mineral. Petrol. Geochem.* **2024**, *43*, 14–34. (In Chinese with English Abstract) [CrossRef]
83. Liu, J.J.; Zheng, M.H.; Liu, J.M.; Lu, W.Q.; Liu, X.F. Au-Se enrichment and accumulation mechanisms in the Cambrian stratabound gold deposits in Jiangzha, western Qinling Mountains. *Geochimica* **2001**, *30*, 155–162. (In Chinese with English Abstract) [CrossRef]
84. Lv, Z.C.; Liu, C.Q.; Liu, J.J.; Zhao, Z.Q. Study on carbon, oxygen and boron isotopes of Ziyang Huangbaishuwan and Zhushan Wenyuhe witherite deposits. *Sci. China* **2003**, *33*, 223–235. [CrossRef]
85. Zhang, W.G.; Li, H.T.; Wang, F.; Yang, P.; Teng, J.X. Solid-liquid migration of molybdenum in stone coal and coal ash in southern Shaanxi. *Coal Geol. Explor.* **2020**, *48*, 64–70. (In Chinese with English Abstract) [CrossRef]
86. Wen, H.J.; Xiao, H.Y. A Review of Selenium Minerals. *Acta Petrol. Mineral.* **1998**, *3*, 260–265. (In Chinese with English Abstract)
87. Zhu, J.M.; Johnson, T.M.; Finkelman, R.B.; Zheng, B.S.; Sykorova, I.; Pesek, J. The occurrence and origin of selenium minerals in Se-rich stone coals, spoils and their adjacent soils in Yutangba, China. *Chem. Geol.* **2012**, *330–331*, 27–38. [CrossRef]
88. Zhu, J.M.; Li, S.H.; Zuo, W.; Sykorova, J.; Su, H.C.; Zheng, B.S.; Pesek, J. Modes of occurrence of selenium in black S-rich rocks of Yutangba. *Geochimica* **2004**, *33*, 634–640. (In Chinese with English Abstract) [CrossRef]
89. Liu, J.J.; Feng, C.X.; Zheng, M.H. The Studying Situation on Selenium Resource and Its Exploiting and Utilizing Prospect. *World Sci.-Tech. R D* **2001**, *16*, 16–21. (In Chinese with English Abstract)
90. Qin, H.B.; Zhu, J.M.; Su, H. Selenium fractions in organic matter from Se-rich soils and weathered stone coal in selenosis areas of China. *Chemosphere* **2012**, *86*, 626–633. [CrossRef] [PubMed]
91. Qu, J.G.; Xu, B.X.; Gong, S.C. Sequential Extraction Techniques for Deter-Mination of Selenium Speciation in Soils and Sediments. *Environ. Chem.* **1997**, *3*, 277–283.
92. Zhu, Z.J.; Guo, F.S. Heavy mineral distribution regularity of Paleogene detrital rocks in Lanping basin, Yunnan Province. *Geol. Bull. China* **2017**, *36*, 199–208. (In Chinese with English Abstract)
93. Morton, A.C.; Hallsworth, C.R. Processes controlling the composition of heavy mineral assemblages in sandstons. *Sediment. Geol.* **1999**, *124*, 3–29. [CrossRef]
94. Wang, G.R.; Chen, H.D.; Zhu, Z.J.; Lin, L.B.; Fan, Y. Characteristics and Geological Implications of Heavy Minerals in Lower Silurian Xiaoheba Formation sandstones in Southeast Sichuan-West Hunan. *J. Chengdu Univ. Technol. Sci. Technol. Ed.* **2011**, *38*, 7–14. (In Chinese with English Abstract)
95. Garzanti, E.; Ando, S. Heavy minerals concentration in modern sands: Implications for provenance interpretation. *Dev. Sedimentol.* **2007**, *58*, 517–545. [CrossRef]
96. Luo, K.L.; Jiang, J.S. Selenium content and enrichment law of Lower Cambrian strata in Ziyang and Langao, Shaanxi. *Geol. Geochem.* **1995**, *23*, 68–71. (In Chinese with English Abstract)
97. Huang, Y.H.; Ren, Y.X.; Xia, L.X.; Xia, Z.C.; Zhang, C. Early Paleozoic bimodal igneous suite on Northern Daba Mountains: Gaotan diabase and Haoping trachyte as examples. *Acta Petrol. Sin.* **1992**, *8*, 243–256. (In Chinese with English Abstract)
98. Zhang, F.Y.; Lai, S.C.; Qin, J.F. Magma source and evolution process of Early Paleozoic basalt in the South Qinling Belt. *Acta Petrol. Sin.* **2020**, *36*, 2149–2162. (In Chinese with English Abstract)

99. Li, Y.H.; Wang, W.Y.; Li, H.R. Environmental behaviors of selenium in soil of typical selenosis area, China. *J. Environ. Sci.* **2008**, *20*, 859–864. [CrossRef]
100. Zheng, B.S.; Yan, L.R.; Mao, D.J.; Su, H.C.; Zhou, H.Y.; Xia, W.P.; Hong, Y.T.; Zhao, W.; Chen, F.; Zhu, X.Q.; et al. The Se Resource in Southwestern Hubei Province, China, and Its Exploitation Strategy. *J. Nat. Resour.* **1993**, *8*, 204–212. [CrossRef]
101. Zhang, C.L.; Gao, S.; Zhang, G.W. Geochemistry of early Paleozoic alkali dyke swarms in south Qinling and its geological significance. *Sci. China* **2003**, *32*, 1292–1306. [CrossRef]
102. Zhu, J.M.; Johnson, T.M.; Clark, S.K.; Zhu, X.K.; Wang, X.L. Selenium redox cycling during weathering of Se-rich shales: A selenium isotope study. *Geochim. Cosmochim. Acta* **2014**, *126*, 228–249. [CrossRef]
103. Mao, D.J.; Su, H.C. Selenium migration and environmental selenium capacity of stone coal in aqueous media. *Bull. Dis. Control. Prev. (China)* **1997**, *3*, 58–59. (In Chinese with English Abstract) [CrossRef]
104. Li, D.P. The Microelement Feature and A Suggestion of Selenium-Rich Crops to be Developed in Ziyang Area. *Geol. Shaanxi* **1999**, *1*, 67–73. (In Chinese with English Abstract)
105. Fan, H.F.; Wen, H.J.; Hu, R.Z. Enrichment of Multiple Elements and Depositional Environment of Selenium-rich Deposits in Yutangba, Western Hubei. *Acta Sedimentol. Sin.* **2008**, *26*, 271–282.
106. Dhillon, K.; Dhillon, S.; Singh, B. Genesis of seleniferous soils and associated animal and human health problems. *Adv. Agron.* **2019**, *154*, 1–80. [CrossRef]
107. Chang, C.; Yin, R.; Zhang, H.; Yao, L. Bioaccumulation and Health Risk Assessment of Heavy Metals in the Soil-Rice System in a Typical Seleniferous Area in Central China. *Environ. Toxicol. Chem.* **2019**, *38*, 1577–1584. [CrossRef] [PubMed]
108. Zhu, J.; Wang, N.; Li, S.; Li, L.; Su, H.; Liu, C. Distribution and transport of selenium in Yutangba, China: Impact of human activities. *Sci. Total Environ.* **2008**, *392*, 252–261. [CrossRef]
109. Karaj, S.; Dhillon, S.; Dhillon, K. Development and mapping of seleniferous soils in northwestern India. *Chemosphere* **2014**, *99*, 56–63.
110. Long, J.; Luo, K.L. Trace element distribution and enrichment patterns of Ediacaran-early Cambrian, Ziyang selenosis area, Central China: Constraints for the origin of Selenium. *J. Geochem. Explor.* **2017**, *172*, 211–230. [CrossRef]
111. Wei, F.S.; Yang, G.Z.; Jiang, D.Z.; Liu, Z.H.; Sun, B.M. Basic Statistics of Background Values of Soil Elements in China. *Environ. Monit. China* **1984**, *7*, 1–6. (In Chinese with English Abstract)
112. Chen, D.Z. Selenium in soil of Shaanxi Region. *Acta Pedol. Sin.* **1984**, *21*, 247–257. (In Chinese with English Abstract)
113. Tan, J.A. *Atlas of Endemic Diseases and Environment in the People's Republic of China*; Science Press: Beijing, China, 1991. (In Chinese with English Abstract)
114. Zhang, J.D.; Wang, L.; Wang, H.D.; Luo, K.L.; Wu, B.C. Distribution of Soil Total Selenium in Ziyang, Shaanxi. *Chin. J. Soil Sci.* **2017**, *48*, 1404–1408. (In Chinese with English Abstract) [CrossRef]
115. Liu, J.B.; Xu, H.G.; Yuan, H.W.; Zhang, X.F. Speciation of selenium in typical meadow soils in Tumed Left Banner, Inner Mongolia, China. *Geophys. Geochem. Explor.* **2024**, *48*, 245–254. (In Chinese with English Abstract)
116. Dinh, T.; Wang, M.K.; Thu, T.A.T.; Zhou, F.; Wang, D.; Zhai, H.; Qin, P.; Xue, M.Y.; Zekun, D.; Gerardo, B.; et al. Bioavailability of selenium in soil-plant system and a regulatory approach. *Crit. Rev. Environ. Sci. Technol.* **2018**, *49*, 1–75. [CrossRef]
117. Tolu, J.; Bouchet, S.; Helfenstein, J.; Hausheer, O.; Chékifi, S.; Frossard, E.; Tamburini, F.; Chadwick, O.A.; Winkel, L.H.E. Understanding soil selenium accumulation and bioavailability through size resolved and elemental characterization of soil extracts. *Nat. Commun.* **2022**, *13*, 6974. [CrossRef] [PubMed]
118. Gan, L.M. *Distribution Characteristics and Influencing Factors of Soil Seleniumin Selenium Abnormal Area in Central Guangxi*; Nanning Normal University: Nanning, China, 2024. (In Chinese with English Abstract)
119. Chen, Y.Z.; Wang, F.; Shan, R.Y.; Chen, C.S.; Yu, W.Q.; You, Z.M. Selenium contents and forms in soils at tea plantations of different soil types in northern Fujian. *Acta Tea Sin.* **2022**, *63*, 243–250. (In Chinese with English Abstract) [CrossRef]
120. Liu, Y.; Jiang, B.; Zhang, H.R.; Sun, Z.B.; Wang, S.T. Study on geochemical background value of soil in Qingzhou City of Shandong Province. *Chin. Agric. Sci. Bull.* **2022**, *4*, 66–71. (In Chinese with English Abstract)
121. Shi, T.C.; Yang, J.F.; Yang, B.G.; Cao, Y.Y.; Ma, G.L. Analysis of selenium content, form and valence in farmland soil of northern Ningxia. *J. Ningxia Univ. Nat. Sci. Ed.* **2022**, *43*, 62–67. (In Chinese with English Abstract)
122. Zhang, Y.F.; Miao, G.W.; Ma, Q.; Ji, B.Y.; Xu, G. Distribution characteristics of Se speciation of alkaline soil in eastern Qinghai. *Geophys. Geochem. Explor.* **2019**, *43*, 1138–1144. (In Chinese with English Abstract)
123. Yang, K.; Li, L.X.; Zhang, J.Y.; Zhang, L.X.; Shang, S.G.; Zhang, Q.M.; Wang, Y.M. Selenium bioavailability and the influential factors in potentially selenium enriched soils in Lujiang county, Anhui Province. *Res. Environ. Sci.* **2018**, *31*, 715–724. (In Chinese with English Abstract) [CrossRef]
124. Li, S.B.; Yang, G.L.; Xiong, W.L.; Ma, Z.C.; Yuan, H.W.; Duan, J.X. Speciation of selenium in the selenium-rich cultivated land in Linhe district, Bayannur city, Inner Mongolia and its influencing factors. *Geophys. Geochem. Explor.* **2023**, *47*, 477–486. (In Chinese with English Abstract) [CrossRef]